

Multifractal behavior of crystallization on Au/Ge bilayer films

Z. W. Chen*

Structure Research Laboratory, University of Science and Technology of China, Hefei 230026, People's Republic of China

X. P. Wang

Department of Physics, University of Science and Technology of China, Hefei 230026, People's Republic of China

S. Tan, S. Y. Zhang, and J. G. Hou

Structure Research Laboratory, University of Science and Technology of China, Hefei 230026, People's Republic of China

Z. Q. Wu

Fundamental Physics Center, University of Science and Technology of China, Hefei 230026, People's Republic of China

(Received 31 March 2000; revised manuscript received 8 December 2000; published 3 April 2001)

The relationship between the distribution and the dimension of fractal patterns in annealed Au/Ge bilayer films has been investigated. The variation of the single-fractal branch width can be shown by using a simple fractal dimension. The nonuniform distribution of multiple-fractal patterns can be described quantitatively by using the multifractal spectra. It has been demonstrated that, when the fractals are fewer, they exhibit the greater nonuniform distribution and the multifractal spectrum is wider. We found that a few fractal patterns distribute nonuniformly in film annealed at 100 °C for 60 min, and that many fractal patterns distribute uniformly in whole film annealed at 120 °C for 60 min. Correspondingly, the width $\Delta\alpha$ of multifractal spectra decreases from 3.70 to 0.23.

DOI: 10.1103/PhysRevB.63.165413

PACS number(s): 68.37.Lp, 81.10.Jt, 61.43.Hv

I. INTRODUCTION

Owing to the sensitive and complex dependence of thin films microstructure and growth conditions, a great deal of attention has been played on the studies of the microstructure and the physical properties.¹⁻⁴ In fact, the self-similar fractal patterns can be formed in metal/amorphous semiconductor (M/a-S) bilayer films during crystallization of the amorphous semiconductor layer in contact with a metal layer.⁵⁻⁸ Since the middle of the 1980s,⁹⁻¹² the relationship between the fractal formation of M/a-S bilayer films, the annealing temperature, the annealing time, the thickness of films, and the electron emission, etc., have been investigated thoroughly. The mechanism of the fractal growth in M/a-S bilayer films have been also proposed by Hou and Wu,³ while the studies of the fractal crystallization mainly focused on the measurement of the single-fractal dimension. However, some studies indicate that the multiple-fractal structure can be formed in the thin solid films.¹³ The distribution of the multiple fractals in whole films cannot be described using a simple fractal dimension. Although the fractal dimension has been used to describe a rough surface,¹⁴ the single-fractal dimension cannot provide enough information.

The multifractal spectra can describe the different gradational characteristics of the fractal structure.¹⁵ The research field is mainly the probability distribution of a few parameters. In the past few years, the multifractals have been found to have important application in electron microscopy. Huang¹⁶ *et al.* have studied the geometrical difference of a fractal cluster by use of the multifractal approach. In their study, they have given an explanation of the information dimension and the correlation dimension. They have declared that the information dimension is related to the cluster

growth mechanism. Li, Ding, and Wu¹⁷ have simulated the spatial distributions of secondary-electron emission sites and secondary-electron emission energies at these Si emission sites by the multifractal spectra in addition to the usual approximate contour map plot. They found that the more non-uniform of the spatial distributions of the secondary-electron emission sites and energies at these Si emission sites is wider for the multifractal spectra. Ohta and Honjo¹⁸ have studied the multifractal spectra of the branched crystal growth, comparing it with the fractal theory. Wang, Wang, and Wu¹⁹ pointed out the multifractal behavior of solid-on-solid growth. They found that the widths $\Delta\alpha$ and the heights Δf of multifractal spectra $f(\alpha)$ are related to the average film thickness h as $\Delta\alpha \sim h^{0.9}$.

In this paper, we present first that the multifractality can characterize the growth process of the Au/a-Ge bilayer films. We found better correlativity between the fractal crystallization and the multifractal spectra in annealed Au/Ge bilayer films. By using multifractal spectra, we can study the subtle geometrical feature of the distribution of the fractal patterns in Au/Ge bilayer films. This method seems to be developed to describe the fractal growth process.

II. EXPERIMENTAL AND MULTIFRACTAL METHOD

Specimens were prepared by evaporation freshly cleaved NaCl (100) crystal in vacuum with a pressure of 2×10^{-5} Torr at room temperature. We deposited Ge at first and then Au without breakout the vacuum (about 2×10^{-5} Torr) by evaporating high-purity germanium (99.9%) and gold (99.9%) from two resistive-heated tungsten boats. The thickness of polycrystalline Au (*p*-Au) and amorphous Ge (*a*-Ge) films are about 25 and 18 nm, respectively. All

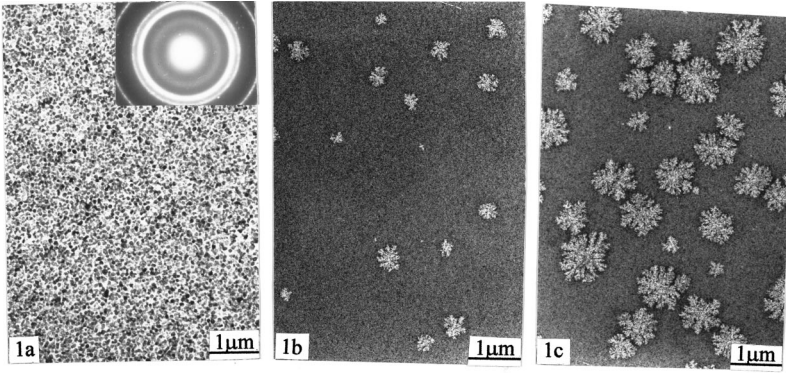


FIG. 1. TEM images of Au/a-Ge bilayer films annealed at 100 °C for (a) 45 min; (b) 60 min; and (c) 70 min.

as-evaporated specimens were annealed in vacuum of about 2×10^{-5} Torr at 100 °C for 45, 60, and 70 min; and 120 °C for 30, 40, and 60 min respectively. After annealing, the specimens were floated on distilled water and then placed on copper meshes to be observed with a HITACHI H-800 Transmission Electron Microscope (TEM) operated at 200 kV.

TEM images were digitized by use of Fractal Images Process Software. The four intact fractal patterns were selected from these digitized images. The fractal dimension (D) average value of four digitized fractal patterns has been carried out by using the Sandbox method.²⁰ These digitized images were divided into boxes of size 360×360 and then were processed by the multifractal method. At first, we have to find the distribution of fractal growth probabilities on the film as follows.

The 360×360 digitized image is divided into boxes of size $m \times m$ (m is the positive integer), let $\varepsilon = m/L$ ($L = 360$) and the distributed probability $P_{ij}(\varepsilon)$ of the fractal patterns in the box (i, j) is defined as

$$P_{ij}(\varepsilon) = \frac{N_{ij}(\varepsilon)}{\sum N_{ij}(\varepsilon)} = \frac{N_{ij}(\varepsilon)}{N}, \quad (1)$$

where $N_{ij}(\varepsilon)$ is the number of pixels for the fractal patterns inside the box (i, j) of size ε , and N the total number of pixels for the fractal patterns inside the largest box, i, j represent the coordinates of the small box along the x, y axes, respectively. Changing the box size at the condition that $360/m$ is an integer, we can find a singular exponent α_{ij} by the following equation:²¹

$$P_{ij}(\varepsilon) \sim \varepsilon^{\alpha_{ij}}. \quad (2)$$

From the partition function $\chi_q(\varepsilon)$ expressed as a power law with an exponent $\tau(q)$, where q is the moment order

$$\chi_q(\varepsilon) = \sum P_{ij}^q(\varepsilon) = \varepsilon^{\tau(q)}, \quad (3)$$

and the generalized fractal dimension D_q

$$D_q = \frac{1}{q-1} \lim_{\varepsilon \rightarrow 0} \frac{\ln \left[\sum_{ij} P_{ij}^q(\varepsilon) \right]}{\ln \varepsilon}, \quad (4)$$

we can obtain $f(\alpha)$ by a Legendre transformation as follows:

$$\alpha = \frac{d}{dq} [(q-1)D_q], \quad (5)$$

and

$$f(\alpha) = \alpha q - (q-1)D_q, \quad (6)$$

that is, the relationship between the multifractal spectra $f(\alpha)$ and α

$$f(\alpha) \sim \alpha. \quad (7)$$

III. RESULTS

Figures 1(a) to 1(c) show the TEM images of the Au/a-Ge bilayer films annealed at 100 °C for various annealing times. For the film annealed at 45 min [Fig. 1(a)] the selected area electron diffraction patterns show several sharp Au rings and two diffuse Ge rings, indicating that the speci-

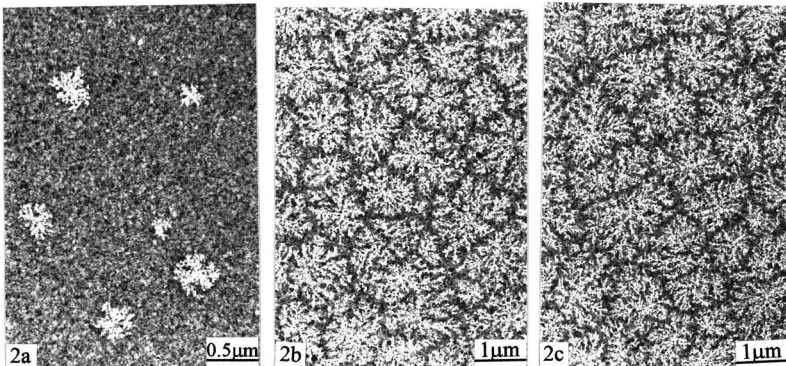


FIG. 2. TEM images of Au/a-Ge bilayer films annealed at 120 °C for (a) 30 min; (b) 40 min; and (c) 60 min.

TABLE I. Fractal dimension (D) and area percent (P) of fractal patterns with various annealing process.

Annealing temperature	Annealing time (min)	Fractal dimension (D)	Area percent (P)
100 °C	60	1.518 ± 0.060	2.5
	70	1.685 ± 0.021	14.6
120 °C	30	1.552 ± 0.014	4.4
	40	1.746 ± 0.026	40.3
	60	1.752 ± 0.028	42.6

men of Au/*a*-Ge bilayer films annealing at 45 min is composed of amorphous Ge and polycrystalline Au. The distribution of Au grain is uniform and no Ge fractal pattern appears here. After annealing from 60 to 70 min, the films present a self-similar fractal patterns. It can be seen from the TEM images that there is a little difference on the fractal density and size for 60 and 70 min annealing specimens. The number of the fractal patterns are less, the difference of the fractal size is large, and the distribution of the fractal patterns is nonuniform for 60 min annealing specimen [Fig. 1(b)]. When the annealing time reached 70 min [Fig. 1(c)], the sizes and the number of the fractal patterns increased, and the distribution of the fractal patterns was also nonuniform.

Figures 2(a) to 2(c) show the TEM images of the Au/*a*-Ge bilayer films annealed at 120 °C for various annealing times. The partial crystallization of Au/*a*-Ge bilayer film began with annealing at 30 min [Fig. 2(a)], and the film appears as a nonuniform and sparse fractal pattern. For the film annealed at 40 min [Fig. 2(b)], the Au/*a*-Ge bilayer film has crystallized completely, the number of the fractal patterns increased swiftly, and the whole film was covered with the uniform fractal patterns. Combining the results presented in Figs. 2(b) and 2(c), it became known that the morphology of the Au/*a*-Ge bilayer film at 60 min annealing [Fig. 2(c)] was similar to that of 40 min annealing. Table I shows the fractal dimension (D) and the area percent (P) of the fractal patterns with various annealing processes. It can be seen that the dimension and number of the fractal patterns increased with the increase in the annealing temperature and time.

Figure 3 shows the $\ln \chi_q$ - $\ln \varepsilon$ plots of the fractal patterns in Au/*a*-Ge bilayer film annealed at 120 °C for 40 min by using the multifractal method. It can be seen that, when $q < -1$, there are two regions, while the segment I and II correspond to the regions of the large ε and the small ε , respectively.

Figures 4(a) and 4(b) show the multifractal spectra of the fractal patterns in Au/*a*-Ge bilayer films annealed at 100 and 120 °C for various annealing times. For the specimen annealed at 100 °C [Fig. 4(a)], the multifractal spectra of the fractal regions are wider at 60 min annealing. When the annealing time reached 70 min, it is evident that the multifractal spectrum is contracted, and the uniformity of the fractal distribution was improved. For the specimen annealed at 120 °C [Fig. 4(b)], the multifractal spectrum is still wider and irregular at 30 min annealing. When the annealing time reached 40 min, the multifractal spectrum is rapidly contracted, and the distribution of the fractal regions is uniform. Combining the results presented in specimens of 60 and 40

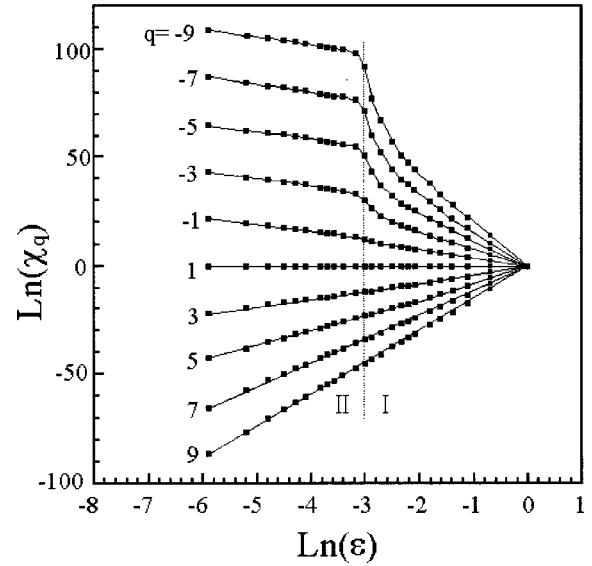


FIG. 3. The $\ln \chi_q$ - $\ln \varepsilon$ plots of fractal patterns in Au/*a*-Ge bilayer film annealed at 120 °C for 40 min.

min annealing, we can find that the multifractal spectrum has been contracted a little for the specimen at 60 min annealing, and the uniformity has been improved a little for the fractal distribution. Table II shows the list of the key parameters of the multifractal spectra of specimen with different annealing processes. Among them is $\Delta\alpha = \alpha_{\max} - \alpha_{\min}$. As seen in Table II, the minimum singularity α_{\min} increase with the increase in the annealing time, and the maximum singularity α_{\max} decrease with the increase in the annealing time.

IV. DISCUSSION

In general, the fractal dimension has been carried out by using the sandbox method,²⁰ area-radius of gyration (S- R_g) method,²² and box-counting method.²³ The sandbox method has been adopted in a fractal dimension analysis of Au/*a*-Ge bilayer films by calculating pixels of fractal regions in a gradual increment box. This method is applied to calculate the simple fractal dimension of the single-fractal pattern, the distribution of the fractal patterns cannot be fully described. The S- R_g method may measure the average dimension of many fractal patterns, which has nothing to do with the distribution of the fractal patterns. The simple box-counting method is applied to process the whole picture of many fractal regions. It does not be considered the pixels differences in the square, and it is still given the simple fractal dimension.

As seen in TEM results, the branches of the fractal patterns become from the sparse to the dense in Au/*a*-Ge bilayer films with increasing annealing temperature and time. The quantitative analysis of these fractal patterns may be described by the average dimension of many fractal patterns (Table I). In order to examine the deep-level characterization of fractal structure in Au/*a*-Ge bilayer films, the multifractal spectra $f(\alpha)$ have been adopted in the distribution of the fractal patterns in the M/*a*-S bilayer films. From the relationship between the probability $P_{ij}(\varepsilon)$ of fractal growth, the fractal dimension, and some multifractal parameters¹⁶ such

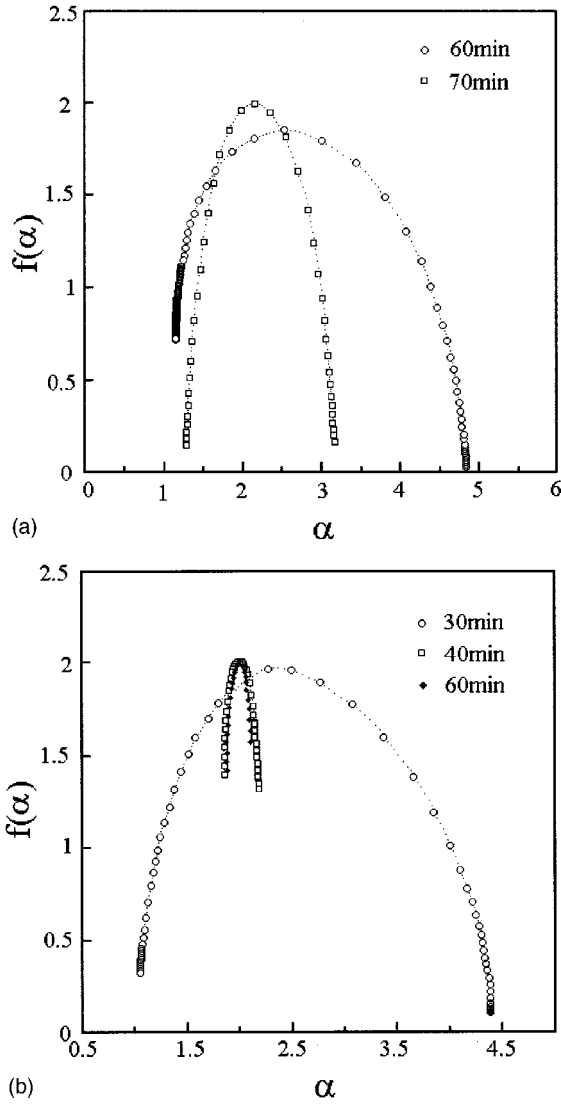


FIG. 4. The multifractal spectra of fractal patterns in Au/a-Ge bilayer film annealed at (a) 100 °C and (b) 120 °C.

as the minimum singularity α_{\min} and the maximum singularity α_{\max} they can be obtained from Eqs. (3)–(5), and the multifractal spectra $f(\alpha)$ from Eq. (6). The multifractal spectra $f(\alpha)$ have been also used to describe the nonuniformity of the fractal patterns, which can provide more information than the simple fractal dimension. The region behavior of the

TABLE II. List of key parameters of the multifractal spectra of specimens with different annealing process.

Annealing temperature	Annealing time (min)	α_{\min}	α_{\max}	$\Delta\alpha$
100 °C	60	1.15	4.85	3.70
	70	1.29	3.17	1.88
120 °C	30	1.06	4.40	3.34
	40	1.86	2.20	0.34
	60	1.88	2.11	0.23

smaller probability can be described using the large α in fractal spectra. The region behavior of the larger probability can be described using the smaller α . The nonuniform distribution of fractal growth probability can be described using the widths $\Delta\alpha$ of multifractal spectra $f(\alpha)$. The large $\Delta\alpha$ indicates the nonuniform distribution of fractal growth probability.

As seen in Fig. 3, the curves obviously consist of two linear segments for $q < -1$ (defined as segments I and II). It is also seen that the shapes of plots for segments I and II are different. The shape for segments I is normal (ϵ larger) and the shape for segments II is anomalous (ϵ smaller). Similar spectra have been observed in the distribution of secondary-electron emission sites on the solid surface.¹⁷ In segments II, the scale invariance is broken down in the smaller probability region and $q < -1$ (in the outer zone of the fractal patterns).²⁴

The $f(\alpha) \sim \alpha$ curves in Fig. 4 show that all of the maximum $f(\alpha)$ are equal to 2 ($f_{\max} = 2$) when the total number of fractal patterns are large enough. In segments I, the width $\Delta\alpha$ of multifractal spectra $f(\alpha)$ decreases with the increasing annealing time at two annealing temperatures (100 and 120 °C). The decrease of $\Delta\alpha$ is caused by the fact that the distribution of fractal growth probability on various annealing time tends to be uniform and that when the total number of fractal patterns are large enough, the dimensions of all specimens with various α are converged to a point (2, 2) in the $f(\alpha) \sim \alpha$ plot. Nakamura¹⁴ studied the fractal property of randomly deposited film on one-dimensional substrate and obtained three Hausdorff dimensions according to three different definitions. Furthermore, he also found that the fractal dimension of small clusters is quite different from that of larger ones. His study can only be used in the case of low coverage, since there will be a few very large clusters if the coverage is large. Compared with our results, the multifractal spectra obtained by us are sensitive and precise enough to describe fractal growth process of Au/a-Ge bilayer films from $\Delta\alpha = 3.70$ to $\Delta\alpha = 0.23$.

These findings support the conclusion that the nonuniform distribution of fractal growth in Au/a-Ge bilayer films can also be described by multifractal analysis in addition to the usual approximate contour map plot. The subtle geometrical difference between the distributions and the fractal structure can be provided by some multifractal parameters. The results of multifractal analysis indicate that the fractal crystallization process in Au/a-Ge bilayer films can be characterized by a multifractal approach, the width $\Delta\alpha$, and the singularity spectra $f(\alpha)$. This means that the widths $\Delta\alpha$ of multifractal spectra $f(\alpha)$ decrease with the increase in the annealing temperature and time, that is, the smaller $\Delta\alpha$ fractal crystallization the better.

V. CONCLUSION

In conclusion, we analyzed the relationship between the distribution and the dimension of fractal patterns in annealed Au/a-Ge bilayer films. It is demonstrated that the fractal crystallization process in annealed Au/a-Ge bilayer films can be characterized by the multifractal approach, the width

$\Delta\alpha$, and singularity spectra $f(\alpha)$. We found that a few fractal patterns distribute nonuniformly in the film annealed at 100 °C for 60 min, and that many fractal patterns distribute uniformly in whole film annealed at 120 °C for 60 min. Correspondingly, the width $\Delta\alpha$ of multifractal spectra decreases from 3.70 to 0.23

ACKNOWLEDGMENTS

J. G. Hou thanks the National Nature Science Foundation of China for financial support. This research was supported by the Structure Research Laboratory, University of Science, and Technology of China.

*Author to whom correspondence should be addressed. FAX: 86-551-360-2803. Electronic address: chenzw@ustc.edu.cn

¹L. Bardotti, P. Jensen, A. Hoareau, M. Treilleux, and B. Cabaud, *Phys. Rev. Lett.* **74**, 4694 (1995).

²G. Deutscher and Y. Lereah, *Phys. Rev. Lett.* **60**, 1510 (1988).

³J. G. Hou and Z. Q. Wu, *Phys. Rev. B* **40**, 1008 (1989); **42**, 3271 (1990).

⁴J. Chevrier and V. Le Thanh, *Europhys. Lett.* **16**, 737 (1991).

⁵S. Alexander, R. Bruinsma, R. Hilfer, G. Deutscher, and Y. Lereah, *Phys. Rev. Lett.* **60**, 1514 (1988).

⁶S. W. Russell, J. Li, and J. W. Mayer, *J. Appl. Phys.* **70**, 5153 (1991).

⁷J. Krim, I. Heyvaert, C. V. Haesendonck, and Y. Bruynseraede, *Phys. Rev. Lett.* **70**, 57 (1993).

⁸S. Wang and P. Halevi, *Phys. Rev. B* **47**, 10 815 (1993).

⁹L. S. Bi and Z. Q. Wu, *Phys. Rev. B* **41**, 11 591 (1990); X. H. Wu, Y. Z. Feng, and Z. Q. Wu, *J. Appl. Phys.* **75**, 2415 (1994).

¹⁰S. Y. Zhang, X. P. Wang, Z. W. Chen, Z. Q. Wu, N. Y. Jin-Phillipp, M. Kelsch, and F. Phillipp, *Phys. Rev. B* **60**, 5904 (1999); X. Zheng and Z. Q. Wu, *Z. Phys. B: Condens. Matter* **73**, 129 (1988).

¹¹Z. W. Chen, S. Y. Zhang, S. Tan, J. G. Hou, and Y. H. Zhang, *J. Vac. Sci. Technol. A* **16**, 2292 (1998); *Thin Solid Films* **322**,

194 (1998).

¹²L. Ba, J. L. Zen, and Z. Q. Wu, *J. Appl. Phys.* **77**, 587 (1995).

¹³Y. Hayakawa, S. Sato, and M. Matsushita, *Phys. Rev. A* **36**, 1963 (1987); T. C. Halsey, M. H. Jensen, L. P. Kadanoff, I. Procaccia, and B. Shraiman, *ibid.* **33**, 1411 (1986).

¹⁴M. Nakamura, *Phys. Rev. B* **41**, 12 268 (1990); **40**, 3358 (1989); **40**, 2549 (1989).

¹⁵A. Sanchez, R. Serna, F. Catalina, and C. N. Afonso, *Phys. Rev. B* **46**, 487 (1992); T. Vicsek, F. Family, and P. Meakin, *Europhys. Lett.* **12**, 217 (1990).

¹⁶L. J. Huang, B. X. Liu, J. R. Ding, and H. D. Li, *Phys. Rev. B* **40**, 858 (1989).

¹⁷H. Li, Z. J. Ding, and Z. Q. Wu, *Phys. Rev. B* **51**, 13 554 (1995); **53**, 16 631 (1996).

¹⁸S. Ohta and H. Honjo, *Phys. Rev. Lett.* **60**, 611 (1988).

¹⁹B. Wang, Y. Wang, and Z. Q. Wu, *Solid State Commun.* **96**, 69 (1995).

²⁰S. R. Forrest and T. A. Witten, *J. Phys. A* **12**, L109 (1979).

²¹A. Chhabra and R. V. Jensen, *Phys. Rev. Lett.* **62**, 1327 (1989).

²²Z. Q. Wu and R. J. Zhang, *Prog. Phys.* **14**, 435 (1994).

²³J. Feder, *Fractal* (Plenum, New York, 1988), p. 15.

²⁴R. Blumenfeld and A. Aharony, *Phys. Rev. Lett.* **62**, 2977 (1989).